
DeepHoyer: Learning Sparser Neural Network with Differentiable Scale-Invariant Sparsity Measures

Huanrui Yang

ECE Department
Duke University
Durham, NC 27708

huanrui.yang@duke.edu

Wei Wen

ECE Department
Duke University
Durham, NC 27708

wei.wen@duke.edu

Hai Li

ECE Department
Duke University
Durham, NC 27708

hai.li@duke.edu

Abstract

In seeking for sparse and efficient neural network models, many previous works investigated on enforcing ℓ_1 or ℓ_0 regularizers to encourage weight sparsity during training. The ℓ_0 regularizer measures the parameter sparsity directly and is invariant to the scaling of parameter values, but it cannot provide useful gradients, and therefore requires complex optimization techniques. The ℓ_1 regularizer is almost everywhere differentiable and can be easily optimized with gradient descent. Yet it is not scale-invariant, causing the same shrinking rate to all parameters, which is inefficient in increasing sparsity. Inspired by the Hoyer measure (the ratio between ℓ_1 and ℓ_2 norms) used in traditional compressed sensing problems, we present DeepHoyer, a set of sparsity-inducing regularizers that are both differentiable almost everywhere and scale-invariant. Our experiments show that enforcing DeepHoyer regularizers can produce even sparser neural network models than previous works, under the same accuracy level. We also show that DeepHoyer can be applied to both element-wise and structural pruning.

1 Introduction

The use of deep neural network (DNN) models has been expanded from handwritten digit recognition [1] to real-world applications, such as large-scale image classification [2], self driving [3] and complex control problems [4]. However, a modern DNN model like AlexNet [5] or ResNet [6] often introduces a large number of parameters and computation load, which makes the deployment and real-time processing on embedded and edge devices extremely difficult [7, 8, 9]. As a result, model compression techniques, especially pruning methods that increase the sparsity of the weight matrices, have been extensively studied to reduce the memory consumption and computation cost of DNNs [7, 8, 9, 10, 11, 12, 13, 14].

Sparsity-inducing regularizers like ℓ_1 or ℓ_0 have long been utilized in searching for sparse neural networks: Liu et al. [14] directly apply ℓ_1 regularization to all the weights of a DNN to achieve element-wise sparsity; while Han et al. [7] enforce an element-wise ℓ_0 constraint over all DNN weights by pruning a certain percent of smallest weight elements in every training iteration. More recently, Wen et al. [9, 15] present structural sparsity via group lasso, which applies an ℓ_1 regularization over the ℓ_2 norms of different groups of parameters. More effective ℓ_0 regularization is also achieved by integrating with stochastic approximation [11] or more complex optimization methods (e.g. ADMM) [13]. Although both ℓ_1 and ℓ_0 based regularizers achieve promising results, each has its own limitations. The ℓ_1 regularizer can be easily optimized through gradient descent benefiting from its convex and almost everywhere differentiable property. However, the value of the ℓ_1 regularizer is proportional to the scaling of the parameters (i.e. $\|\alpha W\|_1 = |\alpha| \|W\|_1$), so it can only “scale down” all the elements in the weight matrices with the same speed. This is not efficient in leading to sparsity,

and will shrink the variance of the parameters throughout the training process, which may sacrifice the flexibility of the trained model. On the other hand, the ℓ_0 regularizer can directly reflect the real sparsity of the weights and is scale invariant (i.e. $\|\alpha W\|_0 = \|W\|_0, \forall \alpha \neq 0$), yet the ℓ_0 norm cannot provide useful gradients, therefore requiring additional measures for optimization [11, 13]. These additional measures brought overheads to the ℓ_0 regularization, making the extension of these methods to larger networks difficult. In seeking for even sparser neural networks, we argue to move beyond ℓ_0 and ℓ_1 regularizers and seek for a sparsity-inducing regularizer that is both almost everywhere differentiable (like ℓ_1) and scale-invariant (like ℓ_0).

Plenty of sparsity measurements have been used in the field of compressed sensing [16]. Hoyer measure, proposed by Patrik O. Hoyer in 2004 [17] is one of them. Hoyer measure estimates the sparsity of a vector with the ratio between its ℓ_1 and ℓ_2 norms. Comparing to using the ℓ_1 norm as sparsity measure, Hoyer measure achieves superior performance and therefore has been widely applied in the fields of non-negative matrix factorization [17], sparse reconstruction [18, 19] and blend deconvolution [20, 21]. We note that the Hoyer measure is both almost everywhere differentiable and scale invariant, satisfying the desired property of a sparsity-inducing regularizer. Inspired by the Hoyer measure, we propose *DeepHoyer*, where we

- Achieve element-wise sparsity by enhancing the original Hoyer regularizer to the Hoyer-Square regularizer and apply it to DNN training. This is the first time Hoyer-inspired regularizers are applied in DNN training;
- Induce structural sparsity by extending the Hoyer-Square regularizer to the Group-HS regularizer;
- Perform extensive experiments with the proposed regularizers on modern DNNs (including ResNet-50 [6]) and beat state-of-the-arts in both element-wise and structural weight pruning of deep neural networks, including those based on ℓ_0 and ℓ_1 regularizers.

2 Related work on DNN pruning

It is well known that high redundancy pervasively exists in deep neural networks. Consequently, pruning methods have been extensively investigated to identify and remove unimportant weights. Some heuristic pruning methods [7, 10] simply remove weights in small values to generate sparse DNN models. These methods usually require long training times while cannot guarantee the optimality due to the lack of theoretical analyses and well-formulated optimization [13]. Some works formulate the problem as a sparsity-inducing optimization problem, such as an ℓ_1 regularization [14, 22] that can be optimized using standard gradient-based algorithms, or an ℓ_0 regularization [11, 13] which requires stochastic approximation or special optimization techniques. We propose the DeepHoyer regularizers in this work, which belong to the line of sparsity-inducing optimization research. More specific, the proposed Hoyer-Square regularizer for element-wise pruning is scale-invariant and can serve as an differentiable approximation to the ℓ_0 norm. Moreover, it can be optimized by gradient-based optimization methods in the same way as the ℓ_1 regularization. With the help of these properties, the Hoyer-Square regularizer achieves a further 96% and 72% sparsity improvement on LeNet-300-100 model and LeNet-5 model respectively comparing to previous state-of-the-arts, and achieves similar sparsity as the more complex ADMM method [13] on AlexNet.

Structurally sparse DNNs have more regular sparse pattern for hardware friendly execution. To achieve the goal, Li et al. [23] apply pruning methods to remove filters with small norms; Wen et al. [9] propose group Lasso regularization based methods to remove various structures (filters, channels, layers and neurons) in DNNs and the similar methods are proposed to remove neurons in [24]; Liu et al. [25] and MorphNet [26] enforce sparsity-inducing regularization on the scaling parameters within Batch Normalization layers, aiming to remove the corresponding channels in DNNs. ThiNet [12] removes unimportant filters by minimizing the reconstruction error of feature maps; and He et al. [27] incorporate both Lasso regression and reconstruction error into the optimization problem. Bayesian optimization methods have also been applied for neuron pruning [28, 29], yet these methods are not applicable in large-scale problems like ImageNet. We further advance the DeepHoyer to learn structured sparsity (such as sparse filters and channels) with assistance of the newly proposed “Group-HS” regularization. The Group-HS regularizer further improves the computation reduction of the LeNet-5 model by 8.8% from the ℓ_1 based method [9] and by 110.6% from the ℓ_0 based method [11]. Moreover, the Group-HS regularizer achieves a $1.89 \times$ computation reduction

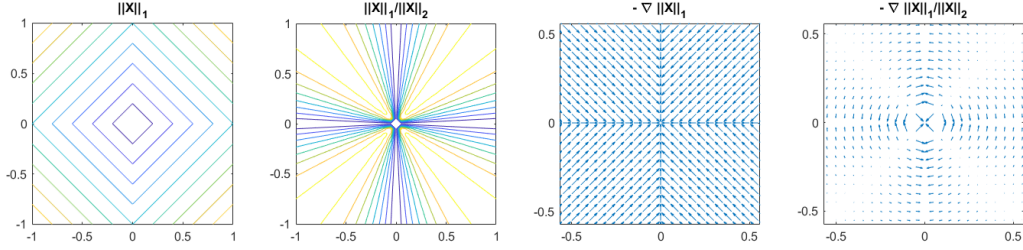


Figure 1: Comparing the ℓ_1 and the Hoyer regularizer of a 2-D vector. Their contours are shown in the left 2 subplots (darker color corresponds to a lower value). The right 2 subplots compare their negative gradients.

on the more compact ResNet-50 model without accuracy loss, which is the highest computation reduction ever achieved without accuracy loss on the ResNet-50 model. More detailed results can be found in Section 5.

3 Measuring sparsity with the Hoyer measure

Sparsity measures have been extensively studied in the compressed sensing research because they provide tractable sparsity constraints for enforcement during problem solving. In early non-negative matrix factorization (NMF) research, a consensus was that a sparsity measure should map a n -dimensional vector to a real number between 0 and 1, where the sparsest possible vectors (with only one nonzero element) have sparsity 1 and the vectors with all elements equal have sparsity 0 [17]. Under such an assumption, the Hoyer measure in Equation (1) was proposed, where n is the dimensionality of vector X .

$$S(X) = \frac{\sqrt{n} - (\sum_i |x_i|) / \sqrt{\sum_i x_i^2}}{\sqrt{n} - 1}. \quad (1)$$

It is obvious that

$$1 \leq \frac{\sum_i |x_i|}{\sqrt{\sum_i x_i^2}} \leq \sqrt{n}, \quad \forall X \in \mathbb{R}^n. \quad (2)$$

Thus, the normalization in Equation (1) fits the measure $S(X)$ into the $[0, 1]$ interval. From a 2009 survey [16], there are six desired heuristic criteria for sparsity measures. The Hoyer measure satisfies five of the six criteria, which is more than any other commonly applied sparsity measure does [16].

Given its success as a sparsity measure in NMF, the Hoyer measure has also been applied as a sparsity-inducing regularizer in optimization problems such as blind deconvolution [21] and image deblurring [20]. Without the range constraint, in these works the Hoyer regularizer takes the form $R(X) = \frac{\sum_i |x_i|}{\sqrt{\sum_i x_i^2}}$ directly, which is the ratio of the ℓ_1 norm and the ℓ_2 norm of the vector X .

Figure 1 demonstrates a comparison of the Hoyer regularizer and the ℓ_1 regularizer. It can be seen that the Hoyer regularizer has minima along the axes, which is very similar to the minima structure of the ℓ_0 norm. In contrast, the ℓ_1 norm has a single minimum at the origin. So the ℓ_1 regularizer cannot identify sparse data points among the points lying in parallel to the ℓ_1 unit ball, while the Hoyer regularizer can [30]. Note that both the ℓ_1 norm and the ℓ_2 norm are proportional to the scaling of X . So the Hoyer regularizer $R(X)$ is scale-invariant, i.e. $R(\alpha X) = R(X)$. The gradients of the Hoyer regularizer are purely radial, leading to “rotations” towards the nearest axis. The similarity of Hoyer regularizer’s minima structure to the ℓ_0 norm’s and the availability of gradient information enables the Hoyer regularizer to outperform the ℓ_1 regularizer on various tasks [18, 19, 20, 21]. The theoretical analysis by Yin et al. [30] also show that the Hoyer regularizer has a better guarantee than the ℓ_1 norm on recovering sparse solutions from coherent and redundant representations.

4 Model compression with DeepHoyer regularizers

We propose two types of DeepHoyer regularizers: the *Hoyer-Square* regularizer for element-wise pruning and the *Group-HS* regularizer for structural pruning. In this section, we will first introduce these two regularizers, then elaborate their usage in neural network pruning tasks.

4.1 Hoyer-Square regularizer for element-wise pruning

The objective of the element-wise DNN pruning is to minimize the ℓ_0 norm of each layer’s weight matrix. Therefore it is a straightforward idea to configure the sparsity-inducing regularizer to have a similar behavior as the ℓ_0 norm. As shown in Inequality (2), the original Hoyer regularizer of a N -dimensional nonzero vector lies between 1 and \sqrt{N} , while its ℓ_0 norm is within the range of $[1, N]$. So we propose to use the square of the Hoyer regularizer, *Hoyer-Square* (H_S), as the regularizer to the weights W of each layer, such as

$$H_S(W) = \frac{(\sum_i |w_i|)^2}{\sum_i w_i^2}. \quad (3)$$

The H_S regularizer now has the same range as the ℓ_0 norm. Moreover, H_S is scale invariant as $H_S(\alpha W) = H_S(W)$ holds for $\forall \alpha \neq 0$, which is the same as the ℓ_0 norm. Because squaring is a monotonously increasing operator in the range of $[1, \sqrt{N}]$, the Hoyer-Square regularizer’s minima remain along the axes as the Hoyer regularizer’s do (see Figure 1), which is similar to the minima structure of the ℓ_0 norm. The Hoyer-Square regularizer is also almost everywhere differentiable. Its gradient w.r.t. an element w_j in the weight matrix W is formulated in Equation (4):

$$\partial_{w_j} H_S(W) = 2\text{sign}(w_j) \frac{\sum_i |w_i|}{(\sum_i w_i^2)^2} \left(\sum_i w_i^2 - |w_j| \sum_i |w_i| \right). \quad (4)$$

Similar to the ℓ_1 norm, the original gradient of $H_S(W)$ is ill-defined at $w_j = 0$. Here we define $\partial_{w_j} H_S(W)|_{w_j=0} = 0$, so the zero elements will not be penalized by the regularizer during the pruning of W . Summing up all these properties, we conclude that the proposed Hoyer-Square regularizer behaves as a differentiable approximation to the ℓ_0 norm.

Equation (4) shows that when $H_S(W)$ is being minimized through gradient descent, the element w_j will move towards 0 if $|w_j| < \frac{\sum_i w_i^2}{\sum_i |w_i|}$, otherwise moves away from 0. In other words, unlike ℓ_1 regularizer which leads to the shrinking of all the elements, our Hoyer-Square regularizer will turn smaller weights to zero while protecting larger weights, and gradually extend the scope of pruning as more weights coming close to zero. This behavior can be observed in the gradient descent path shown in Figure 2. The figure also indicates that the value of the Hoyer-Square regularizer is getting closer to the ℓ_0 norm of the vector throughout the optimization process, proving that the Hoyer-Square regularizer is a good approximation to the ℓ_0 norm.

4.2 Group-HS regularizer for structural pruning

Beyond element-wise pruning, structural pruning [9] is often more preferred as it aims to construct the sparsity in a structured way so as to achieve higher computation speed-up on general computation platforms. The structural pruning is previously empowered by the *group lasso* [31, 9], which is the sum (ℓ_1 norm) of the ℓ_2 norms of all the groups within a weight matrix like

$$R_G(W) = \sum_{g=1}^G \|w^{(g)}\|_2, \quad (5)$$

where $\|W\|_2 = \sqrt{\sum_i w_i^2}$ represents the ℓ_2 norm, $w^{(g)}$ is a group of elements in the weight matrix W and W consists of G such groups.

Following the same approach in Section 4.1, we use the Hoyer-Square regularizer to replace the ℓ_1 regularizer in the group lasso formulation and define the *Group-HS* (G_H) regularizer in Equation (6):

$$G_H(W) = \frac{(\sum_{g=1}^G \|w^{(g)}\|_2)^2}{\sum_{g=1}^G \|w^{(g)}\|_2^2} = \frac{(\sum_{g=1}^G \|w^{(g)}\|_2)^2}{\|W\|_2^2}. \quad (6)$$

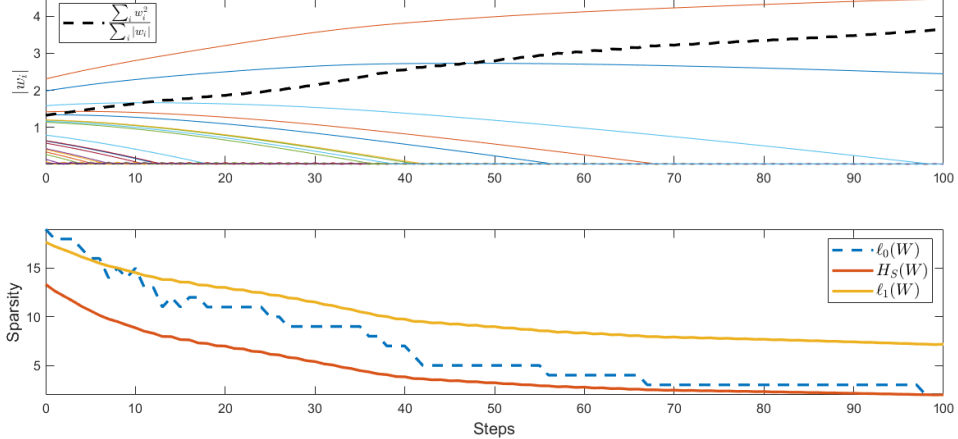


Figure 2: Minimization path of Hoyer-Square regularizer during gradient descent, with $W \in \mathbb{R}^{20}$ initialized as i.i.d. $\mathcal{N}(0, 1)$. Top subfigure shows the path of each element w_i during the minimization, with the black dash line showing the induced threshold deciding whether w_i will be shrunk or preserved by the regularizer. Bottom subfigure compares the change of $H_S(W)$ and $\ell_1(W)$ with the true sparsity measured by $\ell_0(W)$.

Note that the second equality holds when and only when the groups cover all the elements of W without overlapping with each other, which is the case in the experiments in this paper. However, the Group-HS regularizer can always be used in the form of the first equality even if overlapping exists across groups. The gradient and the descent path of the Group-HS regularizer are very similar to those of the Hoyer-Square regularizer, therefore the detailed discussion is omitted here. The derivation of the Group-HS regularizer’s gradient can be found in [Appendix A](#).

4.3 Apply DeepHoyer regularizers in DNN training

We follow the common layer-based regularization approach [9, 14] when applying the DeepHoyer regularizers in DNN training. For element-wise pruning, we apply the Hoyer-Square regularizer to every layer’s weight $W^{(l)}$ of all the L layers, and directly minimize it alongside the DNN’s original training objective $\mathcal{L}(W^{(1:L)})$. The ℓ_2 regularizer can also be added to the objective if needed. Equation (7) presents the modified objective, where H_S is the Hoyer-Square regularizer defined in Equation (3) while α and β are pre-selected weight decay parameters for the regularizers.

$$\min_{W^{(1:L)}} \mathcal{L}(W^{(1:L)}) + \sum_{l=1}^L (\alpha H_S(W^{(l)}) + \beta \|W^{(l)}\|_2). \quad (7)$$

For structural pruning, we mainly focus on pruning the columns and rows of fully connected layers and the filters and channels of convolutional layers. More specific, we group each layer in filter-wise and channel-wise fashion as proposed in [9] and then apply the Group-HS regularizer to the layer. The resulted optimization objective is formulated in Equation (8). Here N_l is the number of filters and C_l is the number of channels in the l^{th} layer if it is a convolutional layer. If the l^{th} layer is fully connected, then N_l and C_l is the number of rows and columns respectively. α_n , α_c and β are pre-selected weight decay parameters for the regularizers.

$$\min_{W^{(1:L)}} \mathcal{L}(W^{(1:L)}) + \sum_{l=1}^L (\alpha_n \frac{(\sum_{n_l=1}^{N_l} \|w_{n_l,:,:,l}^{(l)}\|_2)^2}{\|W^{(l)}\|_2^2} + \alpha_c \frac{(\sum_{c_l=1}^{C_l} \|w_{:,c_l,:,l}^{(l)}\|_2)^2}{\|W^{(l)}\|_2^2} + \beta \|W^{(l)}\|_2). \quad (8)$$

The non-convexity of the regularization function is a potential drawback of the Hoyer regularizer in previous works [20]. This shall not be a big issue when applying the regularizer in a DNN training objective with the help of the recent advance in stochastic gradient descent (SGD) methods that provide satisfying results under large-scale non-convex settings [32, 33], including DNNs with non-convex objectives [34]. Therefore the DeepHoyer regularizers can be directly optimized with

Table 1: Element-wise pruning results on LeNet-300-100 model @ accuracy 98.4%

Method	Nonzero wights left after pruning			
	Total	FC1	FC2	FC3
Orig	266.2k	235.2k	30k	1k
Han [7]	21.8k (8%)	18.8k (8%)	2.7k (9%)	260 (26%)
ADMM [13]	11.6k (4.37%)	9.4k (4%)	2.1k (7%)	120 (12%)
SNIP [37]	13.3k (5.0%)	Not reported in [37]		
Hoyer	6.8k (2.51%)	5.9k (2.50%)	711 (2.37%)	85 (8.50%)
Hoyer-Square	6.2k (2.33%)	5.0k (2.14%)	997 (3.32%)	183 (18.30%)

Table 2: Element-wise pruning results on LeNet-5 model @ accuracy 99.2%

Method	Nonzero wights left after pruning				
	Total	CONV1	CONV2	FC1	FC2
Orig	430.5k	500	25k	400k	5k
Han [7]	36.3k (8%)	330 (66%)	3k (12%)	32k (8%)	950 (19%)
ADMM [13]	6.05k (1.41%)	100 (20%)	2k (8%)	3.6k (0.9%)	350 (7%)
SNIP [37]	8.61k (2.0%)	Not reported in [37]			
Hoyer	4.04k (0.94%)	53 (10.60%)	613 (2.45%)	3.2k (0.81%)	136 (2.72%)
Hoyer-Square	3.55k (0.82%)	67 (13.40%)	848 (3.39%)	2.4k (0.60%)	234 (4.68%)

the same SGD optimizer used for the original DNN training objective. The pruning is conducted following the common three-stage operations: (1) train the DNN with the DeepHoyer regularizer, (2) prune all the weight elements smaller than a predefined small threshold, and (3) finetune the model by fixing all the zero elements and removing the DeepHoyer regularizer.

5 Experiment result

The proposed DeepHoyer regularizers are first tested on the MNIST benchmark using the LeNet-300-100 fully connected model and the LeNet-5 CNN model [1]. We also conduct tests on the ImageNet ILSVRC-2012 benchmark [35] with the AlexNet model [5] and the ResNet-50 model [6]. All the models are implemented and trained in the “PyTorch” deep learning framework [36], where we match the model structure and the benchmark performance with those of previous works for the fairness of the comparison. The experiment results are presented and discussed in rest of this section, which show that the proposed DeepHoyer regularizers consistently outperform previous works in both element-wise and structural pruning. Detailed information on the experiment setups and the parameter choices of our reported results can be found in **Appendix B**.

5.1 Element-wise pruning

Table 1 and Table 2 summarize the performance of the proposed Hoyer-square regularizer on the MNIST benchmark, with comparisons against state of the art element-wise pruning methods. Without losing the testing accuracy, training with the Hoyer-Square regularizer reduces the number of nonzero weights by $42.9\times$ on the LeNet-300-100 model and by $122\times$ on the LeNet-5 model. Among all the existing methods, our method achieves the highest sparsity: it is a 96% improvement on the LeNet-300-100 model and a 72% improvement on the LeNet-5 model comparing to the best-available ADMM [13] method. An ablation study is also done to compare the performance of the Hoyer-Square regularizer with the original Hoyer regularizer. As seen from Table 1 and Table 2, compared to the original Hoyer regularizer, the Hoyer-Square regularizer emphasizes more on the layers with more parameters (i.e. FC1 for both models), while losing the compression performance on smaller layers. Overall, the Hoyer-Square regularizer can achieve the higher compression rate. **Appendix C.1** illustrates the exact effect of the Hoyer-Square regularizer on each layer’s weight distribution.

Table 3: Element-wise pruning results on AlexNet model

Method	Top-5 error increase	#Parameters	Percentage left
Orig	+0.0%	60.9M	100%
Han [7]	-0.1%	6.7M	11.0%
Dynamic surgery [10]	+0.2%	3.45M	5.67%
NeST [38]	-0.1%	3.9M	6.40%
ADMM [13]	+0.0%	2.9M	4.76%
Hoyer-Square	+0.0%	2.89M	4.69%

Table 4: Structural pruning results on LeNet-300-100 model

Method	Accuracy	#FLOPs	Pruned structure
Orig	98.4%	266.2k	784-300-100
Sparse VD [39]	98.2%	67.3k (25.28%)	512-114-72
BC-GNJ [28]	98.2%	28.6k (10.76%)	278-98-13
BC-GHS [28]	98.2%	28.1k (10.55%)	311-86-14
$\ell_{0_{hc}}$ [11]	98.2%	26.6k (10.01%)	266-88-33
Group-HS	98.2%	16.5k (6.19%)	353-45-11

The element-wise pruning performance on the AlexNet model testing on the ImageNet benchmark is presented in Table 3. Without losing the testing accuracy, the Hoyer-Square regularizer achieves a $21.1 \times$ compression rate. Among all previous methods, only the ADMM method [13] can obtain a similar sparsity. Note that the ADMM method requires two additional Lagrange multipliers and involves the optimization of two objectives, while the optimization of the Hoyer-Square regularizer can be directly realized on a single objective without additional variables. In other words, the Hoyer-Square regularizer can achieve a sparse DNN model with a much lower cost. A more detailed layer-by-layer comparison can be found in **Appendix C.2**.

5.2 Structural pruning

In this section, we report the effectiveness of the Group-HS regularizer in structural pruning tasks. Here we mainly focus on the number of neurons (output channels for convolution layers and rows for fully connected layers) left after removing the all-zero channels and rows in the weight matrices. The comparison is then made on the number of float-point operations (FLOPs) needed to inference with the remaining neurons, which indeed represents the potential inference speedup of the pruned model. As shown in Table 4, training with the Group-HS regularizer can reduce the number of FLOPs

¹No results available on ImageNet-level datasets

Table 5: Structural pruning result on LeNet-5 model

Method	Accuracy	#FLOPs	Pruned structure	Scaled to ImageNet
Orig	99.2%	2293k	20-50-800-500	
Sparse VD [39]	99.0%	660.2k (28.79%)	14-19-242-131	Yes
GL [9]	99.0%	201.8k (8.80%)	3-12-192-500	Yes
SBP [29]	99.1%	212.8k (9.28%)	3-18-284-283	No ¹
BC-GNJ [28]	99.0%	282.9k (12.34%)	8-13-88-13	No ¹
BC-GHS [28]	99.0%	153.4k (6.69%)	5-10-76-16	No ¹
$\ell_{0_{hc}}$ [11]	99.0%	390.7k (17.04%)	9-18-26-25	No ¹
Group-HS	99.0%	169.9k (7.41%)	5-12-139-13	Yes

Table 6: Structural pruning result on the ResNet-50 model. A “N/A” is marked if no data is available from the original paper. The “A-D” represent different weight decay parameters of the Group-HS regularizer, which are specified in **Appendix B**.

Model	Top-1 acc	Top-5 acc	#Para reduction	#FLOPs reduction
Orig	76.15%	92.87%	1.00 \times	1.00 \times
Channel pruning [27]	N/A	90.80%	N/A	2.00 \times
ThiNet-70 [12]	72.04%	90.67%	1.51 \times	1.58 \times
ThiNet-50 [12]	71.01%	90.02%	2.06 \times	2.26 \times
ThiNet-30 [12]	68.42%	88.30%	2.95 \times	3.51 \times
Group-HS-A	76.43%	93.07%	1.46 \times	1.89 \times
Group-HS-B	75.20%	92.52%	2.19 \times	3.09 \times
Group-HS-C	73.19%	91.36%	2.98 \times	4.68 \times
Group-HS-D	71.08%	90.21%	3.33 \times	5.48 \times

by $16.2\times$ for the LeNet-300-100 model with a slight accuracy drop. This is the highest speedup among all existing methods achieving the same testing accuracy. Table 5 shows that the Group-HS regularizer can reduce the number of FLOPs of the LeNet-5 model by $12.4\times$, which outperforms most of the existing work—an 8.8% increase from the ℓ_1 based method [9] and a 110.6% increase from the ℓ_0 based method [11]. Only the Bayesian compression method with the group-horseshoe prior (BC-GHS) [28] achieves a higher speedup in this task. However, the Bayesian approach limits BC’s capability to be applied in ImageNet-level problems; while the effectiveness of the Group-HS regularizer can be extended to larger datasets like ImageNet, as we shall show in the following.

We test the pruning effect of the Group-HS regularizer on the ResNet-50 model using the ImageNet dataset. ResNet models have been widely applied in computer vision tasks given its higher performance. The model structure is highly compact, so there haven’t been much promising pruning results on the ResNet models. As shown in Table 6, the Group-HS regularizer can achieve a $1.89\times$ computation reduction without losing accuracy. The computation reduction can be further increased to $3.09\times$ when slightly relaxing the top-5 accuracy loss (less than 0.5%). If a higher compression rate is preferred, the Group-HS regularizer can achieve a $4.68\times$ computation reduction at the top-5 accuracy of 91.36%, which further improves the compression rate of the channel pruning method [27] by $2.23\times$ with 0.56% gain in the accuracy. It also achieves a $5.48\times$ computation reduction at 90.21% top-5 accuracy, which improve the compression rate of the ThiNet-50 model [12] by $2.42\times$ meanwhile enhancing the accuracy 0.19%.

6 Conclusions

In this work, we propose *DeepHoyer*, a set of sparsity-inducing regularizers that are both scale-invariant and almost everywhere differentiable. We show that the proposed regularizers have similar range and minima structure as the ℓ_0 norm, so it can effectively measure and regularize the sparsity of the weight matrices of DNN models. Meanwhile, the differentiable property enables the proposed regularizers to be optimized with standard gradient-based methods, in the same way as the ℓ_1 regularizer is. In the element-wise pruning experiment, the proposed Hoyer-Square regularizer achieves a 96% sparsity increase on the LeNet-300-100 model and a 72% sparsity increase on the LeNet-5 model without accuracy loss comparing to the state-of-the-art. A $21.1\times$ model compression rate is achieved on AlexNet, which can only be achieved previously by adding additional variables and using dual training objectives. In the structural pruning experiment, the proposed Group-HS regularizer further reduces the computation load by 61.7% from the state-of-the-art on LeNet-300-100 model. It also achieves a 8.8% increase from the ℓ_1 based method and a 110.6% increase from the ℓ_0 based method of the computation reduction rate on the LeNet-5 model. On ImageNet, we test the Group-HS regularizer on the more challenging ResNet-50 model, where it achieves a $1.89\times$ computation reduction without losing accuracy, and a $3.09\times$ computation reduction with top-5 accuracy loss less than 0.5%. This cannot be matched by any previous works. These results prove that the DeepHoyer regularizers are effective in achieving both element-wise and structural sparsity in deep neural networks, and can produce even sparser DNN models than previous works.

References

- [1] Yann LeCun, Léon Bottou, Yoshua Bengio, and Patrick Haffner. Gradient-based learning applied to document recognition. *Proceedings of the IEEE*, 86(11):2278–2324, 1998.
- [2] Karen Simonyan and Andrew Zisserman. Very deep convolutional networks for large-scale image recognition. *arXiv preprint arXiv:1409.1556*, 2014.
- [3] Konstantinos Makantasis, Konstantinos Karantzalos, Anastasios Doulamis, and Nikolaos Doulamis. Deep supervised learning for hyperspectral data classification through convolutional neural networks. In *2015 IEEE International Geoscience and Remote Sensing Symposium (IGARSS)*, pages 4959–4962. IEEE, 2015.
- [4] Volodymyr Mnih, Koray Kavukcuoglu, David Silver, Alex Graves, Ioannis Antonoglou, Daan Wierstra, and Martin Riedmiller. Playing atari with deep reinforcement learning. *arXiv preprint arXiv:1312.5602*, 2013.
- [5] Alex Krizhevsky, Ilya Sutskever, and Geoffrey E Hinton. Imagenet classification with deep convolutional neural networks. In *Advances in neural information processing systems*, pages 1097–1105, 2012.
- [6] Kaiming He, Xiangyu Zhang, Shaoqing Ren, and Jian Sun. Deep residual learning for image recognition. In *Proceedings of the IEEE conference on computer vision and pattern recognition*, pages 770–778, 2016.
- [7] Song Han, Jeff Pool, John Tran, and William Dally. Learning both weights and connections for efficient neural network. In *Advances in neural information processing systems*, pages 1135–1143, 2015.
- [8] Song Han, Huizi Mao, and William J Dally. Deep compression: Compressing deep neural networks with pruning, trained quantization and huffman coding. *arXiv preprint arXiv:1510.00149*, 2015.
- [9] Wei Wen, Chunpeng Wu, Yandan Wang, Yiran Chen, and Hai Li. Learning structured sparsity in deep neural networks. In *Advances in neural information processing systems*, pages 2074–2082, 2016.
- [10] Yiwen Guo, Anbang Yao, and Yurong Chen. Dynamic network surgery for efficient dnns. In *Advances In Neural Information Processing Systems*, pages 1379–1387, 2016.
- [11] Christos Louizos, Max Welling, and Diederik P Kingma. Learning sparse neural networks through l_0 regularization. *arXiv preprint arXiv:1712.01312*, 2017.
- [12] Jian-Hao Luo, Jianxin Wu, and Weiyao Lin. Thinet: A filter level pruning method for deep neural network compression. In *Proceedings of the IEEE international conference on computer vision*, pages 5058–5066, 2017.
- [13] Tianyun Zhang, Shaokai Ye, Kaiqi Zhang, Jian Tang, Wujie Wen, Makan Fardad, and Yanzhi Wang. A systematic dnn weight pruning framework using alternating direction method of multipliers. In *Proceedings of the European Conference on Computer Vision (ECCV)*, pages 184–199, 2018.
- [14] Baoyuan Liu, Min Wang, Hassan Foroosh, Marshall Tappen, and Marianna Pensky. Sparse convolutional neural networks. In *Proceedings of the IEEE Conference on Computer Vision and Pattern Recognition*, pages 806–814, 2015.
- [15] Wei Wen, Yuxiong He, Samyam Rajbhandari, Minjia Zhang, Wenhan Wang, Fang Liu, Bin Hu, Yiran Chen, and Hai Li. Learning intrinsic sparse structures within long short-term memory. *arXiv preprint arXiv:1709.05027*, 2017.
- [16] Niall Hurley and Scott Rickard. Comparing measures of sparsity. *IEEE Transactions on Information Theory*, 55(10):4723–4741, 2009.
- [17] Patrik O Hoyer. Non-negative matrix factorization with sparseness constraints. *Journal of machine learning research*, 5(Nov):1457–1469, 2004.
- [18] Ernie Esser, Yifei Lou, and Jack Xin. A method for finding structured sparse solutions to nonnegative least squares problems with applications. *SIAM Journal on Imaging Sciences*, 6(4):2010–2046, 2013.
- [19] Armenak Petrosyan Tran, Clayton Webster, et al. Reconstruction of jointly sparse vectors via manifold optimization. *arXiv preprint arXiv:1811.08778*, 2018.
- [20] Dilip Krishnan, Terence Tay, and Rob Fergus. Blind deconvolution using a normalized sparsity measure. In *CVPR 2011*, pages 233–240. IEEE, 2011.
- [21] Audrey Repetti, Mai Quyen Pham, Laurent Duval, Emilie Chouzenoux, and Jean-Christophe Pesquet. Euclid in a taxicab: Sparse blind deconvolution with smoothed ℓ_1/ℓ_2 regularization. *IEEE signal processing letters*, 22(5):539–543, 2015.
- [22] Jongsoo Park, Sheng Li, Wei Wen, Ping Tak Peter Tang, Hai Li, Yiran Chen, and Pradeep Dubey. Faster cnns with direct sparse convolutions and guided pruning. *arXiv preprint arXiv:1608.01409*, 2016.
- [23] Hao Li, Asim Kadav, Igor Durdanovic, Hanan Samet, and Hans Peter Graf. Pruning filters for efficient convnets. *arXiv preprint arXiv:1608.08710*, 2016.

- [24] Jose M Alvarez and Mathieu Salzmann. Learning the number of neurons in deep networks. In *Advances in Neural Information Processing Systems*, pages 2270–2278, 2016.
- [25] Zhuang Liu, Jianguo Li, Zhiqiang Shen, Gao Huang, Shoumeng Yan, and Changshui Zhang. Learning efficient convolutional networks through network slimming. In *Proceedings of the IEEE International Conference on Computer Vision*, pages 2736–2744, 2017.
- [26] Ariel Gordon, Elad Eban, Ofir Nachum, Bo Chen, Hao Wu, Tien-Ju Yang, and Edward Choi. Morphnet: Fast & simple resource-constrained structure learning of deep networks. In *Proceedings of the IEEE Conference on Computer Vision and Pattern Recognition*, pages 1586–1595, 2018.
- [27] Yihui He, Xiangyu Zhang, and Jian Sun. Channel pruning for accelerating very deep neural networks. In *Proceedings of the IEEE International Conference on Computer Vision*, pages 1389–1397, 2017.
- [28] Christos Louizos, Karen Ullrich, and Max Welling. Bayesian compression for deep learning. In *Advances in Neural Information Processing Systems*, pages 3288–3298, 2017.
- [29] Kirill Neklyudov, Dmitry Molchanov, Arsenii Ashukha, and Dmitry P Vetrov. Structured bayesian pruning via log-normal multiplicative noise. In *Advances in Neural Information Processing Systems*, pages 6775–6784, 2017.
- [30] Penghang Yin, Ernie Esser, and Jack Xin. Ratio and difference of l1 and l2 norms and sparse representation with coherent dictionaries. *Commun. Inform. Systems*, 14(2):87–109, 2014.
- [31] Ming Yuan and Yi Lin. Model selection and estimation in regression with grouped variables. *Journal of the Royal Statistical Society: Series B (Statistical Methodology)*, 68(1):49–67, 2006.
- [32] Ilya Sutskever, James Martens, George Dahl, and Geoffrey Hinton. On the importance of initialization and momentum in deep learning. In *International conference on machine learning*, pages 1139–1147, 2013.
- [33] Diederik P Kingma and Jimmy Ba. Adam: A method for stochastic optimization. *arXiv preprint arXiv:1412.6980*, 2014.
- [34] Peter Auer, Mark Herbster, and Manfred K Warmuth. Exponentially many local minima for single neurons. In *Advances in neural information processing systems*, pages 316–322, 1996.
- [35] Olga Russakovsky, Jia Deng, Hao Su, Jonathan Krause, Sanjeev Satheesh, Sean Ma, Zhiheng Huang, Andrej Karpathy, Aditya Khosla, Michael Bernstein, Alexander C. Berg, and Li Fei-Fei. ImageNet Large Scale Visual Recognition Challenge. *International Journal of Computer Vision (IJCV)*, 115(3):211–252, 2015.
- [36] Adam Paszke, Sam Gross, Soumith Chintala, Gregory Chanan, Edward Yang, Zachary DeVito, Zeming Lin, Alban Desmaison, Luca Antiga, and Adam Lerer. Automatic differentiation in pytorch. In *NIPS-W*, 2017.
- [37] Namhoon Lee, Thalaiyasingam Ajanthan, and Philip Torr. SNIP: SINGLE-SHOT NETWORK PRUNING BASED ON CONNECTION SENSITIVITY. In *International Conference on Learning Representations*, 2019.
- [38] Xiaoliang Dai, Hongxu Yin, and Niraj K. Jha. Nest: A neural network synthesis tool based on a grow-and-prune paradigm. *CoRR*, abs/1711.02017, 2017.
- [39] Dmitry Molchanov, Arsenii Ashukha, and Dmitry Vetrov. Variational dropout sparsifies deep neural networks. In *Proceedings of the 34th International Conference on Machine Learning-Volume 70*, pages 2498–2507. JMLR. org, 2017.

A Derivation of DeepHoyer regularizers' gradients

In this section we provide detailed derivation of the gradient of the Hoyer-Square regularizer and the Group-GS regularizer w.r.t. an element w_j in the weight matrix W .

The gradient of the Hoyer-Square regularizer is shown in Equation (9). The formulation shown in Equation (4) is achieved at the end of the derivation.

$$\begin{aligned}
\partial_{w_j} H_S(W) &= \frac{[\partial_{w_j}((\sum_i |w_i|)^2)] \sum_i w_i^2 - [\partial_{w_j}(\sum_i w_i^2)] (\sum_i |w_i|)^2}{(\sum_i w_i^2)^2} \\
&= \frac{2[\partial_{w_j}(|w_j|)] \sum_i |w_i| \sum_i w_i^2 - 2w_j (\sum_i |w_i|)^2}{(\sum_i w_i^2)^2} \\
&= 2 \frac{\sum_i |w_i|}{(\sum_i w_i^2)^2} (sign(w_j) \sum_i w_i^2 - sign(w_j) |w_j| \sum_i |w_i|) \\
&= 2sign(w_j) \frac{\sum_i |w_i|}{(\sum_i w_i^2)^2} (\sum_i w_i^2 - |w_j| \sum_i |w_i|).
\end{aligned} \tag{9}$$

The gradient of the Group-HS regularizer is shown in Equation (10). For simplicity we use the form shown in the second equality of Equation (6), where there is no overlapping between the groups. Here we assume that w_j belongs to group $w^{(\hat{g})}$.

$$\begin{aligned}
\partial_{w_j} G_H(W) &= \partial_{w_j} \frac{(\sum_{g=1}^G \|w^{(g)}\|_2)^2}{\sum_i w_i^2} \\
&= \frac{[\partial_{w_j}((\sum_{g=1}^G \|w^{(g)}\|_2)^2)] \sum_i w_i^2 - [\partial_{w_j}(\sum_i w_i^2)] (\sum_{g=1}^G \|w^{(g)}\|_2)^2}{(\sum_i w_i^2)^2} \\
&= \frac{2[\partial_{w_j}(\|w^{(\hat{g})}\|_2)] \sum_{g=1}^G \|w^{(g)}\|_2 \sum_i w_i^2 - 2w_j (\sum_{g=1}^G \|w^{(g)}\|_2)^2}{(\sum_i w_i^2)^2} \\
&= 2 \frac{\sum_{g=1}^G \|w^{(g)}\|_2}{(\sum_i w_i^2)^2} \left(\frac{w_j}{\|w^{(\hat{g})}\|_2} \sum_i w_i^2 - w_j \sum_{g=1}^G \|w^{(g)}\|_2 \right) \\
&= 2 \frac{w_j}{\|w^{(\hat{g})}\|_2} \frac{\sum_i |w_i|}{(\sum_i w_i^2)^2} (\sum_i w_i^2 - \|w^{(\hat{g})}\|_2 \sum_{g=1}^G \|w^{(g)}\|_2).
\end{aligned} \tag{10}$$

B Detailed experiment setup

B.1 MNIST experiments

The MNIST dataset [1] is a well known handwritten digit dataset consists of grey-scale images with the size of 28×28 pixels. The whole dataset can be found at <http://yann.lecun.com/exdb/mnist/>, and can be directly accessed with the dataset API provided in the “torchvision” python package (<https://pytorch.org/docs/master/torchvision/datasets.html#mnist>). In our experiments we use the whole 60,000 training set images for the training and the whole 10,000 testing set images for the evaluation. All the accuracy results reported in the paper are evaluated on the testing set. Both the training set and the testing set are normalized to have zero mean and variance one. Adam optimizer [33] with learning rate 0.001 is used throughout the training process. All the MNIST experiments are done with a single TITAN XP GPU.

Both the LeNet-300-100 model and the LeNet-5 model are firstly pretrained without the sparsity-inducing regularizer, where they achieve the testing accuracy of 98.4% and 99.2% respectively. Then the models are further trained for 250 epochs with the DeepHoyer regularizers applied in the objective. The weight decay parameters (α in Equation (7) and (8)) are picked by hand to reach the best result. In the last step, we prune the weight of each layer with threshold proportional to the standard derivation of each layer’s weight. The threshold/std ratio is chosen to achieve the highest sparsity without accuracy loss. All weight elements with a absolute value smaller than the threshold

Table 7: Hyper parameter used for MNIST benchmarks

Model	LeNet-300-100			LeNet-5	
	Regularizer	Decay	Threshold/std	Decay	Threshold/std
Hoyer	0.02	0.04		0.01	0.08
Hoyer-Square	0.0002	0.02		0.0001	0.03
Group-HS	0.002	0.8		0.1	0.008

is set to zero and is fixed during the final finetuning. The pruned model is finetuned for another 100 steps without DeepHoyer regularizers and the best testing accuracy achieved is reported. Detailed parameter choices used in achieving the reported results are listed in Table 7.

B.2 ImageNet experiments

The ImageNet dataset is a large-scale color-image dataset containing 1.2 million images of 1000 categories [35], which has long been utilized as an important benchmark on image classification problems. In this paper, we use the “ILSVRC2012” version of the dataset, which can be found at <http://www.image-net.org/challenges/LSVRC/2012/nonpub-downloads>. We use all the data in the provided training set to train our model, and use the provided validation set to evaluate our model and report the testing accuracy. We follow the data reading and preprocessing pipeline suggested by the official PyTorch ImageNet example (<https://github.com/pytorch/examples/tree/master/imagenet>). For training images, we first randomly crop the training images to desired input size, then apply random horizontal flipping and finally normalize them before feeding them into the network. Validation images are first resized to 256×256 pixels, then center cropped to desired input size and normalized in the end. We use input size 227×227 pixels for experiments on the AlexNet, and input size 224×224 for experiments on the ResNet-50. All the models are optimized with the SGD optimizer [32], and the batch size is chosen as 256 for all the experiments. Two TITAN XP GPUs are used in parallel for the AlexNet training and four are used for the ResNet-50 training. One thing worth noticing is that the AlexNet model provided in the “torchvision” package (<https://github.com/pytorch/vision/blob/master/torchvision/models/alexnet.py>) is not the ordinary version used in previous works [7, 9, 13]. Therefore we reimplement the AlexNet model in PyTorch for fair comparison. We pretrain the implemented model for 90 epochs and achieve 20.4 % top-5 error. The ResNet-50 architecture and pretrained model provided in the “torchvision” package is directly utilized, which achieves 23.85% top-1 error and 7.13% top-5 error.

In the AlexNet experiment, the reported result in Table 3 is achieved by applying the Hoyer-Square regularizer with decay parameter 1e-6. Before the pruning, the model is firstly train from the pretrained model with the Hoyer-Square regularizer for 90 epochs, where an initial learning rate 0.001 is used. An ℓ_2 regularization with 1e-4 decay is also applied. We then prune the convolution layers with threshold 1e-4 and the FC layers with threshold equal to $0.5 \times$ of their standard derivations. The model is then finetuned until the best accuracy is reached. For the ResNet-50 experiments, all the reported results in Table 6 are achieved with 90 epochs of training with the Group-HS regularizer from the pretrained model using initial learning rate 0.1. All the models are pruned with 1e-4 as threshold and finetuned to the best accuracy. The only difference is the Group-HS regularizer’s decay parameter used, where result A is achieved with decay 1e-5, B with decay 2e-5, C with decay 4e-5 and D with decay 5e-5.

C Additional experiment results

C.1 Weight distribution at different stage

Here we demonstrate how will the weight distribution change in each layer at different stages of our element-wise pruning process. Since most of the weight elements will be zero in the end, we only plot the histogram of *nonzero* weight elements for better observation. The histogram of each layer of the LeNet-300-100 model and the LeNet-5 model are visualized in Figure 3 and Figure 4 respectively. It can be seen that majority of the weights will be concentrated near zero after applying

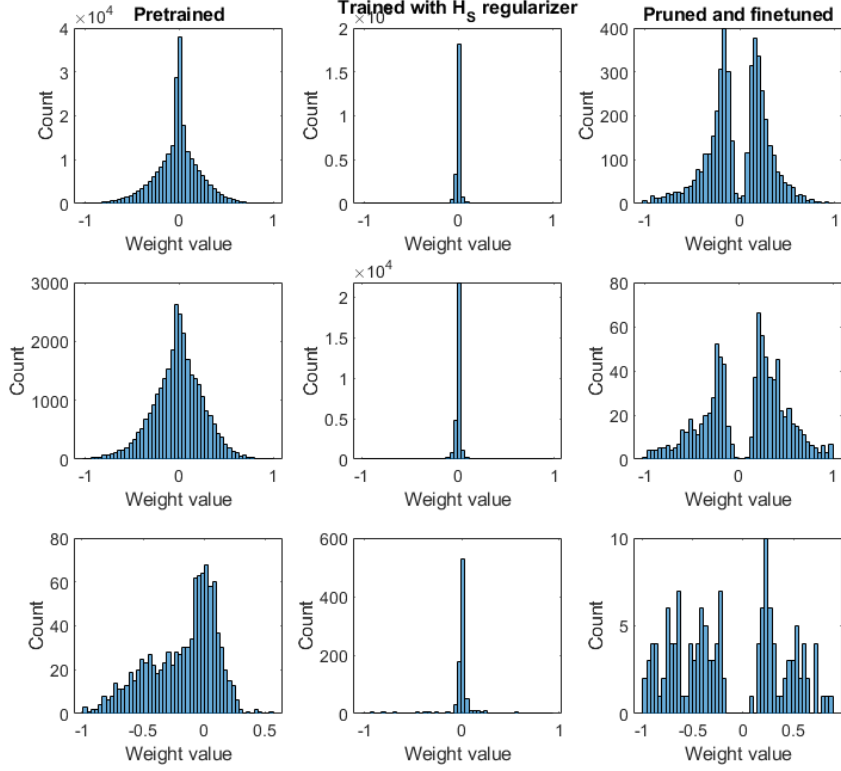


Figure 3: Histogram of *nonzero* weight elements of each layer in the LeNet-300-100 model. From top to bottom corresponds to layer FC1, FC2, FC3 respectively. The original pretrained model is shown in column 1, column 2 shows the model achieved after H_S regularization, column 3 shows the final model after pruning and finetuning.

Table 8: Element-wise pruning results on AlexNet without accuracy loss

Layer	Nonzero weights left after pruning			
	Baseline	Han [7]	ADMM [13]	Hoyer-Square
CONV1	34.8K	29.3K (84%)	28.2K (81%)	29.9K (85.92%)
CONV2	307.2K	116.7K (38%)	61.4K (20%)	157.9K (51.40%)
CONV3	884.7K	309.7K (35%)	168.1K (19%)	303.8k (34.34%)
CONV4	663.5K	245.5K (37%)	132.7K (20%)	240.2k (36.20%)
CONV5	442.2K	163.7K (37%)	88.5K (20%)	174.1k (39.35%)
FC1	37.7M	3.40M (9%)	1.06M (2.8%)	0.769M (2.04%)
FC2	16.8M	1.51M (9%)	0.99M (5.9%)	0.699M (4.17%)
FC3	4.1M	1.02M (25%)	0.38M (9.3%)	0.519M (12.66%)
Total	60.9M	6.8M (11%)	2.9M (4.76%)	2.89M (4.75%)

the H_S regularizer during training, while rest of the weight elements will spread out in a wide range. The weights close to zero are then set to be exactly zero, and the model is finetuned with zero weights fixed. The resulted histogram shows that most of the weights are pruned away, only a small amount of nonzero weights are remaining in the model.

C.2 Layer-by-layer comparison of element-wise pruning result of AlexNet

Table 8 compares the element-wise pruning result of the Hoyer-Square regularizer on AlexNet with other methods in a layer-by-layer fashion. It can be seen that the Hoyer-Square regularizer achieves

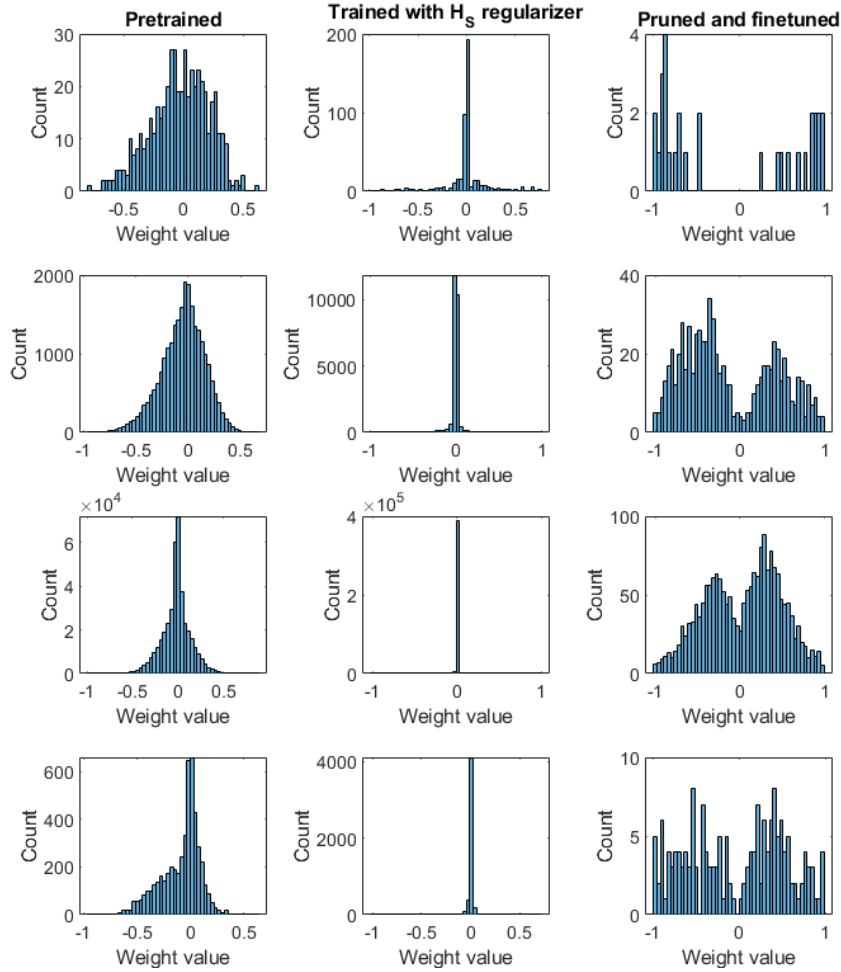


Figure 4: Histogram of *nonzero* weight elements of each layer in the LeNet-5 model. From top to bottom corresponds to layer CONV1, CONV2, FC1, FC2 respectively. The original pretrained model is shown in column 1, column 2 shows the model achieved after H_S regularization, column 3 shows the final model after pruning and finetuning.

the highest pruning rates on the largest layers (i.e. FC1 and FC2). This observation is consistent with the observation made on the element-wise pruning performance of models on the MNIST dataset.